OUTFLOW DYNAMICS, ACCRETION AND CHEMICAL ABUNDANCES IN YSOS

A. Fuente

Observatorio Astronómico Nacional, Apdo. 1143, E-28800 Alcalá de Henares (Madrid), Spain

Abstract

During the last decade, a big improvement has been done in the comprehension of the low-mass star formation. In particular, the large millimetre telescopes and interferometers have provided important information on the physics and chemistry of infall, outflow (shocks) and photodissociation regions (PDRs). However, key details on how low- and intermediate-mass stars are formed remain still unknown (when bipolar outflow starts?, when the collapse ceases? what determines the mass of the star?, when the PDR is formed?, which is the dominant mechanism in the dispersal of the envelope and accretion disk?...). In this paper we discuss how FIRST observations can contribute to a better understanding of these processes. In particular, we consider that oxygen chemistry (H_2O, OH, OI) will constitute an excellent diagnostic for the infall/outflow system. The observation of hydrides will trace the physics and kinematics of the PDRs formed in the later stages of the pre-main sequence evolution. These diagnostics, when applied to statistical studies, could provide the answer to previous questions and a detailed evolutionary sequence for the star formation.

Key words: Stars: formation – Stars: pre-main sequence – ISM: jets and outflows – ISM: clouds – ISM: molecules

1. Introduction

Stars are formed by fragmentation and collapse of dense interstellar clouds. Star formation begins when a dense ($\sim 10^4$ cm^{-3}) and cold (~ 10 K) fragment collapses forming an hydrostatic core surrounded by a massive envelope which hides the central object. This object is called a collapsing pre-stellar core. Eventually powerful stellar winds are developed. These highly obscured objects which already present signs of stellar activity (energetic outflows, continuum emission at cm wavelengths,..) are called protostars. Very young protostars which are so deeply embedded in the parent core that are only detected at mm and sub-mm wavelengths, are called Class 0 protostars. When part of the envelope has been dispersed by the outflow, the protostar becomes detectable in the near-infrared and it is called a Class I protostar (see Figure 1 for an illustrative scheme). In about $\sim 10^6$ yr, the envelope has been dispersed and the star becomes visible (Class II). Once the star is visible, we can talk of a pre-main sequence star. During their evolution to the main-sequence, pre-main sequence stars also disperse the surrounding material by the effect of the stellar winds and photodissociation by the UV stellar radiation evolving from Class II to Class III objects. Eventually, a planetary system could be formed from the remnant circumstellar disk.

The evolution of the circumstellar material during the first stages of the stellar evolution, Class 0 and Class I objects, is dominated by two processes: infall by which the star accretes material onto the central object, and outflow by which the star disperse the surrounding envelope. In the later stages of the pre-main sequence stellar evolution,

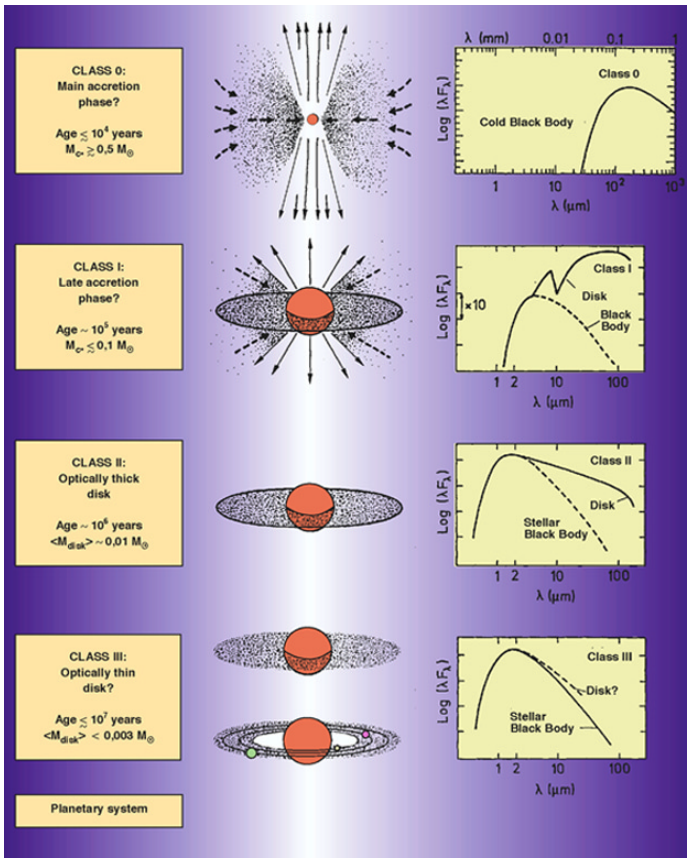

Figure 1. Schematic illustration of the formation and evolution of a low-mass star (modified from Andre et al. 2000).

Proc. Symposium *'The Promise of the Herschel Space Observatory'* 12–15 December 2000, Toledo, Spain
ESA SP-460, July 2001, eds. G.L. Pilbratt, J. Cernicharo, A.M. Heras, T. Prusti, & R. Harris

Class II and Class III objects, the dominant process is the dispersal of the circumstellar matter by the stellar winds and photodissociation. In the following sections, we will discuss how FIRST can improve our understanding of these processes.

2. Class 0 and I objects

2.1. Infall

So far, studies on infall are based mainly on the observation of millimetre lines (see e.g. Myers et al. 2000). These lines trace mainly the outer part of the collapsing envelope ($r > 10^{16}$ cm) in which the collapse velocity is $v_{collapse} < 1$ km s^{-1}. The collapse in the inner region of the envelope and disk is poorly known. Although the spatial resolution provided by present instrumentation is not enough to resolve this region, important information can be obtained from the observation of molecular lines with different excitation conditions and chemistry. For this aim, the observation of the far and mid-infrared lines of CO and H_2O is crucial.

Several models have been developed for a collapsing envelope. Most of them follow the spherical collapse of Shu 1977 which assumes that cores begin the collapse from an initial isothermal equilibrium state in which the gas density law is $n \propto r^{-2}$ .Ceccarelli et al. 1996 modeled the infrared and submillimeter line spectrum produced by the infalling gas around low-mass protostars assuming the collapse model of Shu 1977 and including chemistry, thermal balance and radiative transfer. This model predicts that high H_2O abundances are achieved in the inner region of the envelope ($r \leq 10^{15}$ cm and $T_{dust} > 100$ K) because of the evaporation of the icy grain mantles and endothermic gas-phase reactions. In this region, cooling is mainly by the H_2O lines. In the intermediate region (10^{15} cm $\leq r \leq 10^{16}$ cm) with $T_{dust} \sim 50 - 100$ K, the cooling is mainly by the [OI] 63 μm line. In the outer region ($r > 10^{16}$ cm, $T_{dust} < 50$ K) cooling is dominated by the CO rotational lines. Figure 2 shows the predicted CO line fluxes for a collapsing protostar accreting at 10^{-5} M$_\odot$ yr^{-1} at different times from the start of the collapse. Because of the different excitation conditions, the CO lines can be associated with a characteristic radius (R_{max}) in which most of the flux arises. Figure 2 shows R_{max} for the different transitions to be observed by HIFI. While actual CO studies are based on the millimeter lines ($J < 3$) which trace the external part of the collapsing clump ($r \sim 10^{17}$ cm), the far-infrared high-J transitions observed by HIFI will allow the study of deep inside the collapsing clump to a depth of $\sim 10^{15}$ cm.

During all the protostellar evolution infall and outflow occur simultaneously. One of the main problems for the detection and observational study of infall is the confusion with the emission arising in the shocks produced by the energetic outflow. Furthermore, the evolution of both phenomena is similar. The most energetic phase of

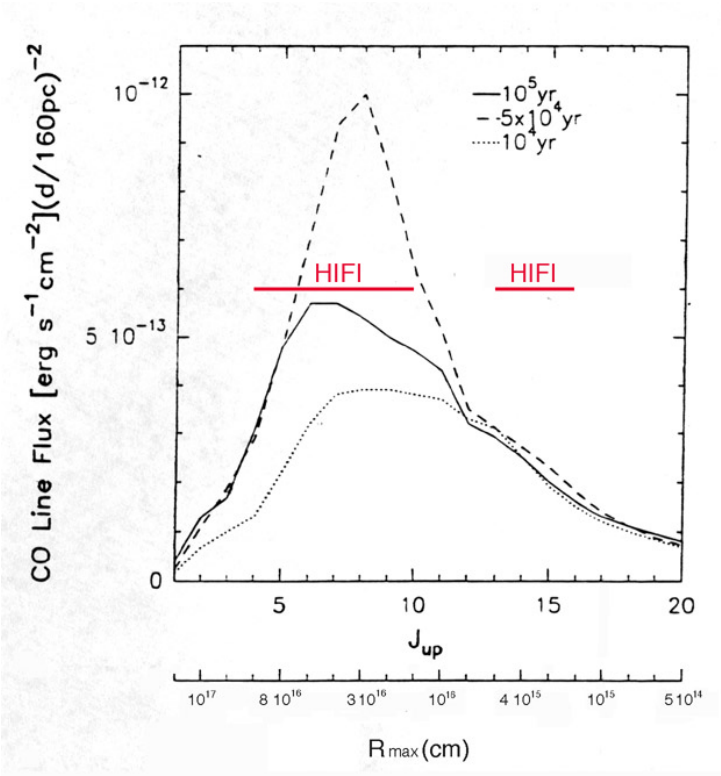

Figure 2. CO line intensities predicted for a protostar accreting at 10^{-5} $M_\odot$ yr^{-1} at 10^4 yr (dotted line), 5×10^4 yr (dashed line), and 10^5 yr (solid line) from the start of the collapse (Ceccarelli et al. 1996). Fluxes are normalized for a source at a distance of 160 pc. The abcisas axis at the bottom indicates the radius at which most of the emission arises.

the outflow takes place during the main accretion phase. The mass accretion rate decreases from $\sim 10^{-6}$ $M_\odot$ yr^{-1} to 10^{-8} $M_\odot$ yr^{-1} and the ratio between the luminosity of the outflow and the bolometric luminosity (L_{out}/L_{bol}) decreases by one order of magnitude when the protostar evolves from Class 0 to Class I. Thus, the search for criteria to distinguish between infall and outflow is essential for the correct interpretation of the data. In Figure 3 we compare the predicted CO fluxes for a collapsing envelope located at a distance of 160 pc, with those predicted by shock models for a typical range of initial densities and shock velocities, assuming that the beam filling factor of the collapsing and shocked regions are similar. Infall dominates the emission in a wide range of low and medium-J transitions (J< 11). However this result is strongly dependent on the assumed source distance and the beam filling factor of the shocked region. Since the collapse is expected to be restricted to the region closest to the star ($r \leq 5\ 10^{16}$ cm), the CO fluxes decreases with the square of the distance. Thus, for a source located at a distance of ~ 500 pc, the fluxes for the infall in Figure 3 should be decreased by an order of magnitude. The beam filling factor of the shocked emission might even increase with the dis-

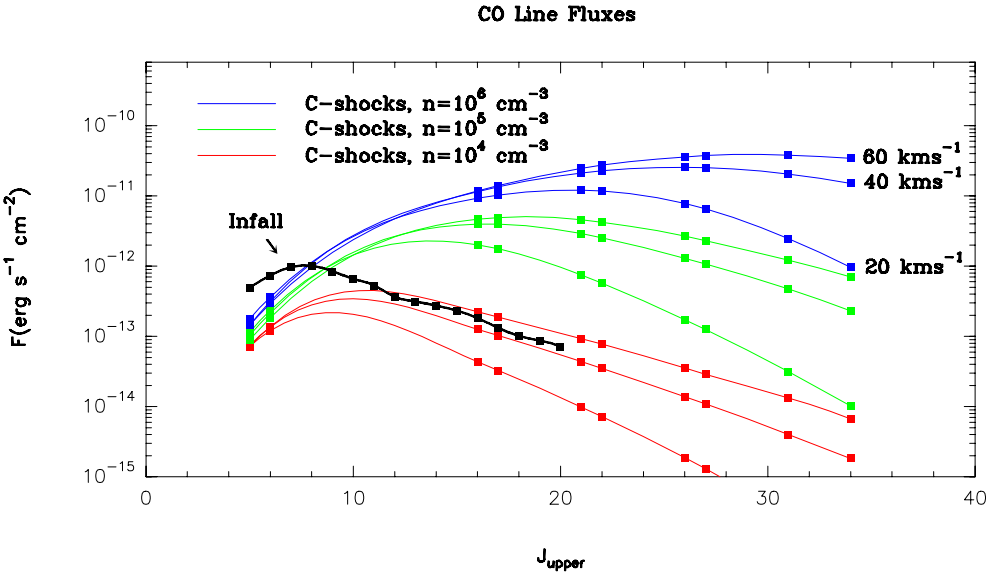

Figure 3. CO fluxes for a protostar accreting at 10^{-5} $M_\odot$ yr^{-1} at 10^4 yr normalized at a distance of 160 pc (black line)(Ceccarelli et al. 1996). In blue, red and green, it is shown the CO fluxes predicted by the models of Kaufman & Neufeld 1996 for the shock emission for thhe range of densities and shock velocities typically found in molecular outflows.

tance depending on the morphology and structure of the outflow. In order to increase the chances of detecting and studying the emission arising in the collapsing envelope, it is essential to choose **nearby and very young objects with highly collimated outflows**. Of course the angular resolution of the observations is also a crucial point. FIRST will provide a Half Power Beam Width (HPBW) a factor of ~ 4 lower than ISO, increasing by a factor of ~ 20 the sensitivity for the infall emission with the same instrumental and observational conditions.

Even in the most favorable case, both the infalling gas and the shocked gas associated with the ouflow will contribute to the observed fluxes. The study of the velocity profile of the lines is one of the most powerful tools to distinguish between infall and outflow. The emission of the outflow is expected to arise in the post-shock gas with velocities close to the outflow velocity which is typically of several tenths of km s^{-1} in Class 0 objects. Even in the inner region of the collapsing envelope, the collapse velocity is below 20 km s^{-1}. The spectral resolution provided by HIFI will be crucial to disetangle between these two phenomena. The excitation of CO and the spatial distribution of the emission can also help to determine the origin of the CO emission. While CO excitation temperatures larger than > 1000 K are found in energetic dense shocks, excitation temperatures of only a few hundreds of K are expected in infalling gas. Furthermore, while outflows associated with young objects are known to have a bipolar morphology and extends over several arcminutes, the collapse is expected to be restricted to a small region around the star. The large number of H_2O lines observable with HIFI, together with the OH and OI lines (HIFI+PACS) will allow the study for the first time the oxygen chemistry. In following sections we will discuss how chemistry, in particular oxygen chemistry, will become one of the main tools to distinguish between infall and outflow and study their structure and evolution.

2.2. Outflows

Outflows are essential for star formation. In particular, outflows carry away the excess of angular momentum from the contracting molecular cloud, and limit the mass and size of the protostellar infalling condensation. Protostars (Class 0 and I objects) produce powerful bipolar outflows which are observable over a wide range of wavelengths, from the UV to the radio showing the wide range of kinetic temperatures (10 to $>$ 1000 K) of the outflowing gas. The shocks produced by bipolar outflows drives a strongly time-dependent shock chemistry with very different characteristics from that of the ambient molecular cloud. Many processes influence the chemical abundances in shocks: (i) Destruction of refractory grain cores in fast shocks,(ii) evaporation of grain mantles in fast or slow shocks, and (iii) the gas-phase endothermic reactions produced in the gas layers compressed and heated by the shock. The last generation of large millimetre telescopes and millimetre interferometers has allowed the detailed mapping of molecular outflows in the wide sample of millimetre molecular lines and the study of the shock chemistry associated with these phenomena.

Bachiller et al. 2001 have carried out a chemical study of L1157 using single-dish and interferometric observations at mm wavelengths. This study includes millimetre observations of about 50 different lines of 27 species. Figure 4 shows the maps of the integrated line intensi-

ties of some molecular lines along the blue lobe of the L 1157 outflow. Comparing the chemical abundances in the star envelope and the outflow, they show that while some species are only detected in the star envelope (see C_3H_2, DCO^+ and N_2H^+ in Figure 4), significantly enhanced abundances, by a factor $\geq$ 50, of SiO, CH_3OH, H_2CO, CS, SO, H_2CS, H_2S and HCN are found along the outflow. Specially interesting is the case of SiO which is detected in the outflow with an abundance enhanced **by a factor $> 10^5$** (see also Martín-Pintado et al. 1992, Schilke et al. 1997). In most cases, these enhancements can be explained as the consequence of the evaporation of the grain mantles and the destruction of the refractory grain cores, giving rise to a chemistry similar to that of a hot core. Significant chemical differences are also found between different positions of the outflow. The different spatial distribution of the sulphur-bearing molecules (SO, SO_2 OCS, H_2S) along the outflow has been interpreted as due to time-dependent chemistry. This is consistent with chemical models which predicts that SO/H_2S and SO_2/SO can be used as chemical clocks (Charnley 1997).

However, the most important molecule which is expected to be enhanced in shock chemistry, H_2O, cannot be observed from ground-based observatories.

2.3. Oxygen chemistry: H_2O

Water is expected to be an important oxygen reservoir in the Universe. In cold clouds, where $T_{dust} < 100$ K, H_2O is formed by the dissociative recombination of H_3O^+. The gas phase H_2O abundance in these regions is expected to be $< 10^{-6}$ since most of the water is locked in the icy grain mantles. In hot regions where $T_{dust} > 100$ K, the icy grain mantles evaporate and H_2O is released to the gas phase. In these regions, the H_2O abundance depends on the fraction of the evaporated H_2O ice. Assuming that 10% of the H_2O ice is evaporated, the water abundance should be $\sim 5\ 10^{-5}$. For higher temperatures, > 200 K, H_2O is formed in gas phase by the endothermic reactions $O + H_2 \rightarrow OH + H$; $H_2 + OH \rightarrow H_2O + H$ and H_2O abundance could be such as high as $\sim 5\ 10^{-4}$, i.e., essentially all the oxygen is locked in H_2O vapour. These high temperatures are found in shocks and photodissociation regions (PDRs). Since H_2O is easily photodissociated by UV radiation, its abundance is expected to remain low ($< 10^{-6}$) in photodissociation regions (PDRs) and dissociative shocks. The H_2O abundance becomes larger than 10^{-4} only in non-dissociative shocks becoming an excellent tracer of these regions. In PDRs and dissociative shocks OI is the dominant oxygenated coolant.

The first works on water have been hampered by the large absorption of the terrestrial atmosphere. Observations from ground based telescopes have been restricted to maser emission and the observation of the rarer isotope $H_2{}^{18}O$. The H_2O maser at 22 GHz has been widely observed in star forming regions, usually associated with young stellar objects (YSOs) and energetic outflows. Cernicharo et al. 1994, 1996 and González-Alfonso et al. 1995 observed the weak maser at 183 GHz towards a sample of massive star forming regions and shocks deriving abundances $\sim 10^{-5}$. Submillimiter maser lines of H_2O have also been observed by Menten et al. 1990. Zmuidzinas et al. 1994 observed the 547 GHz line of $H_2{}^{18}O$ towards Sgr B2 and estimated a water abundance of $< 10^{-7}$ consistent with the low water abundance expected in the cool interstellar medium. Observations of the high excitation lines of $H_2{}^{18}O$ at 203 GHz and 391 GHz towards hot cores, implies water abundance $\sim 10^{-5}$ in these warm regions (Gensheimer et al. 1996). These pioneering results suffer from large uncertainties in the estimate of the H_2O abundance because most of them were based on only one line, and were restricted to a very low number of objects.

The observation of the water transitions between 150 - 200 μm by the ISO-LWS instrument constituted an important input for the knowledge of the oxygen chemistry. Table 1 summarizes the ISO-LWS water observations towards YSOs. Although enhanced water abundances are found in all of them, the high water abundances expected in outflows ($\sim 10^{-4}$) are only found towards L1448 and Orion IRC 2. Observed H_2O abundances seem to be somewhat lower than those predicted by theory. Most of these observations were interpreted as arising in outflows, but Ceccarelli et al. 1999 argue that the H_2O fluxes observed in IRAS+16293-2422 and Elias 29 were also consistent as arising in a collapsing envelope. The poor spatial resolution ($\sim 80''$) and spectral resolving power ($\sim$ 30 - 1500 kms^{-1}) of the observations prevent us from differentiating between infall and outflow. Moreover, since all the observed lines are optically thick and low excitation lines were not observed, the abundance estimates are very uncertain.

Table 1. Summary of the results obtained from the ISO-LWS observations of the water lines between 150–200 μm in young stellar objects.

Source	X(H_2O)	In/out	Ref[1]
IRAS+16293-2422	$\sim 3\ 10^{-6}$	In	(1)
Elias 29	$> 3\ 10^{-6}$	In	(1)
L1448	$\sim 5\ 10^{-4}$	Out	(2)
HH7-11	$\sim 6\ 10^{-6}$	Out	(3)
HH54B	$\sim 10^{-5}$	Out	(4)
Sgr B2	$\sim 10^{-5}$	Out	(5)
Orion IRC2	$\sim 10^{-4}$	Out	(5)

References: (1) Ceccarelli et al. 1999;(2) Nisini et al. 1999; (3) Molinari et al. 2000; (4) Liseau et al. 1996; (5)Cernicharo et al. 1999

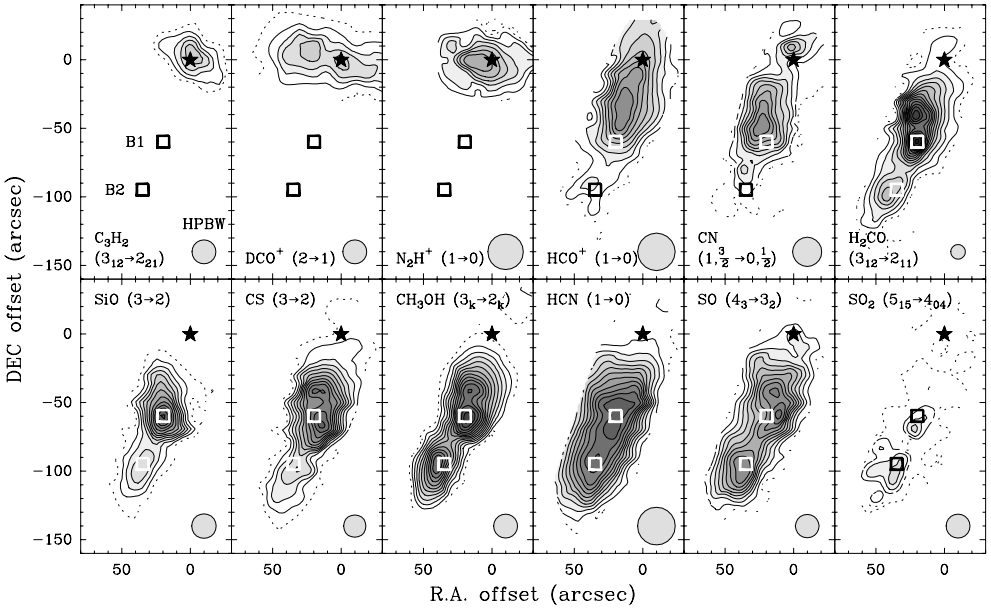

Figure 4. Map of the integrated line intensities of different molecular lines in the L1157 outflow obtained at the IRAM 30-m telescope. Strong chemical effects are found along the outflow (taken from Bachiller et al. 2001).

SWAS has allowed the observation of the ground level 557 GHz line towards a sample of energetic bipolar outflows (NGC 2071, L1157 and NGC 1333 IRAS 4) with high spectral resolution (< 1 km s^{-1}) (see Figure 5)(Neufeld et al. 2000). These observations show that most of the emission arises at the high velocities of the bipolar outflow. However, the poor spatial resolution ($\sim 4'$) and the observation of only one line make it very difficult to have a good estimate of the water abundance in these outflows.

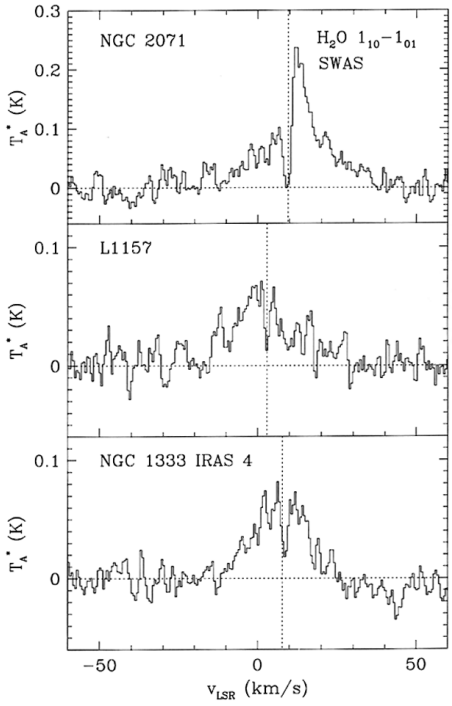

Figure 5. Spectra obtained toward three outflow sources by SWAS showing emission in the H_2O 1_{10} – 1_{01} transition (taken from Neufeld et al. 2000).

3. Class II and III objects

3.1. Herbig Ae/Be stars: PDRs and shocks

In a typical time of 10^7 yr a low mass star disperses the surrounding envelope. Recent millimeter surveys in continuum and line emission show that this time decreases to $< 10^6$ yr for intermediate mass stars (Fuente et al. 1998). The envelope dispersal could be due to the effect of the energetic stellar winds and/or the photodissociation of the gas by the UV radiation. In fact, the mechanism which dominates the envelope dispersal is very likely dependent on the spectral type of the star. The effect of the stellar UV radiation is expected to be much more important in early-type stars.

Herbig Ae/Be stars are a good example of stars in which a mixture of PDRs and shocks are found. Recently, van den Ancker 1999 have observed a large number of Herbig Ae/Be stars with the ISO-SWS instrument. He used the rotational temperature of H_2 to distinguish between PDRs and shocks. High H_2 rotation temperatures (≥ 1000 K) are only expected in non-dissociative shocks. In addition, he used some chemical diagnostics based on the atomic and ionic lines. Specifically, the [SiII] 34.8 μm and [FeII] 26μm lines seem associated with PDRs while the [SI] 25.2 μm becomes detectable only in shocks.

Lorenzetti et al. 1999 observed also a sample of Herbig Ae/Be stars with the ISO-LWS and used the [OI]63

μm and [CII] 158 μm lines to differentiate between PDRs and shocks. The molecular lines (CO, OH, H_2O) were only detected towards the sources with higher densities which are usually associated with bipolar outflows. Comparing the luminosity of the molecular lines with the mechanical luminosity of the outflow in a wide sample of stellar objects, Saraceno et al. 1999 found a general trend with shocks being the main excitation mechanism in Class 0 and low-luminosity Class I objects, and PDRs in the high-luminosity Class I objects and the more massive Herbig Ae/Be stars.

In spite of these encouraging results, these studies suffer from the poor angular and spectral resolution, and limited sensitivity of the ISO-LWS observations. The lack of spatial resolution is dramatic for the more massive Herbig Be stars in which clustering is significant. In fact, outflows in principle associated with a Herbig Ae/Be, are now known to be driven by younger infrared companions (Fuente et al. 2001, Goran & Weintraub et al. 1994). The lack of spectral resolution prevents us from distinguing outflows and PDRs using kinematic arguments even in the case that only one young stellar object is in our beam. In addition, because of the limited sensitivity and poor spatial resolution, even the most abundant molecular species (CO, H_2O and OH) have been detected only in the youngest and densest objects. As we will discuss in the following section, molecular chemistry is a powerful tool for the study and characterization of PDRs.

4. Chemistry of PDRs

PDRs are regions whose structure, chemistry, thermal balance and evolution is determined by the incident FUV field (6eV $<$ hν $<$ 13.6 eV). A PDR is characterized by the incident FUV field (G_0) and the density, n. In the PDRs associated with recently formed stars, the values of G_0 ranges typicaly from 10^2 to $\geq 10^6$, and densities from $\sim 10^3$ to 10^7 cm^{-3}. Although dependent on the ratio G_0/n, the PDR is characterized by a layer of atomic hydrogen that extends to a depth $A_v \sim 1 - 2$ mag from the ionization front, a layer of C^+ that extends to a depth $A_v \sim 2 - 4$ mag and a layer of atomic oxygen that extends to a depth $A_v \sim 10$ mag. Although PDRs are usually associated with atomic gas, some molecular species reach significant abundances in these regions. It is worthy to mention the case of some reactive ions and radicals. These compounds are destroyed rapidly in the interstellar medium by reactions with the most abundant species (H_2, H, e^-, C^+) and their abundances are only significant in the atomic layers of PDRs. Important reactive ions like CO^+, H_3^+,..., and radicals like CH, CH_2, OH,.. belong to this group. Because of this peculiar chemistry, these species constitute an excellent PDR diagnostic (Sternberg & Dalgarno 1995, Black 1998). Chemical studies of prototypical PDRs based on millimeter and submillimeter lines have been carried out during the last years. These observational works confirm that CO^+, HCO^+ and CN have enhanced abundances in PDRs and show that the CN/HCN and CO^+/HCO^+ abundance ratio constitute excellent tracers of these strongly irradiated regions (NGC 2023: Fuente et al. 1995; NGC 7023: Fuente & Martín-Pintado 1997, Orion Bar: Hogerheijde et al. 1995, M17: Latter et al. 1993). Figure 6 shows the observations of the CO^+ N= 2$\rightarrow$1 and HCO^+ J=1$\rightarrow$0 lines towards the prototypical reflection nebula NGC 7023. The CO^+/HCO^+ abundance ratio increases by more than a factor 100 from the shifted molecular cloud to the peak of the PDR. Unfortunately, the most abundant reactive ions and radicals (CH,CH^+,...) do not present observable transitions at millimeter wavelengts. This is the case of hydrides which are expected to have abundances such as high as $\sim 10^{-7} - 10^{-6}$. However, the low rotational transitions of these light compounds lie at far-infrared wavelenghts and cannot be observed from ground-based telescopes.

The launch of ISO allowed for the first time the observation of the pure rotational transitions of H_2, and consequently the measurement of the total amount of warm gas, in PDRs. Because of the limited sensitivity and poor spatial resolution of the ISO-LWS observations, the rotational lines of hydrides were only detected towards the most intense sources. The low number of detections prevented us from carrying out a chemical study of PDRs. FIRST will bring a significant improvement to this situation. To illustrate this situation, we will discuss with some detail the case of the prototypical nebula NGC 7023. The ISO-SWS and LWS observations of this nebula have been reported by Fuente et al. 2000 and Fuente et al. 1999. Six H_2 rotational transitions were observed with fluxes consistent as arising in a PDR with $G_0 \sim 10^4$ and n = 10^6 cm^{-3} and a ortho-to-para H_2 ratio increasing from $\sim$ 1.5 to 3 across the photodissociation region. No molecular species apart from H_2 were detected in this prototypical nebula. In a rough estimate, assuming the physical conditions derived from the H_2 rotational lines, we obtain that in one hour of integration time with FIRST (PACS + HIFI) all the species shown in red in Table 2 will be detectable with a S/N $\sim$ 5. Some other species like CN or CO^+ will be more easily detectable at millimeter wavelengths. Both, millimeter and infrared observations will allow a complete characterization of the chemistry in PDRs.

Recent observations have show that non-stationary effects are important in PDRs (e.g. NGC 7023: Fuente et al. 1999, Lemaire et al. 1999). The thermal structure of the PDR is strongly affected by the advection of molecular gas through the PDR, increasing the mass of warm gas (Bertoldi & Draine 1995, Störzer & Hollenbach 1998). High spectral resolution is essential to study these non-stationary ionization and photodissociation fronts. HIFI will be an essential instrument in the study of PDRs.

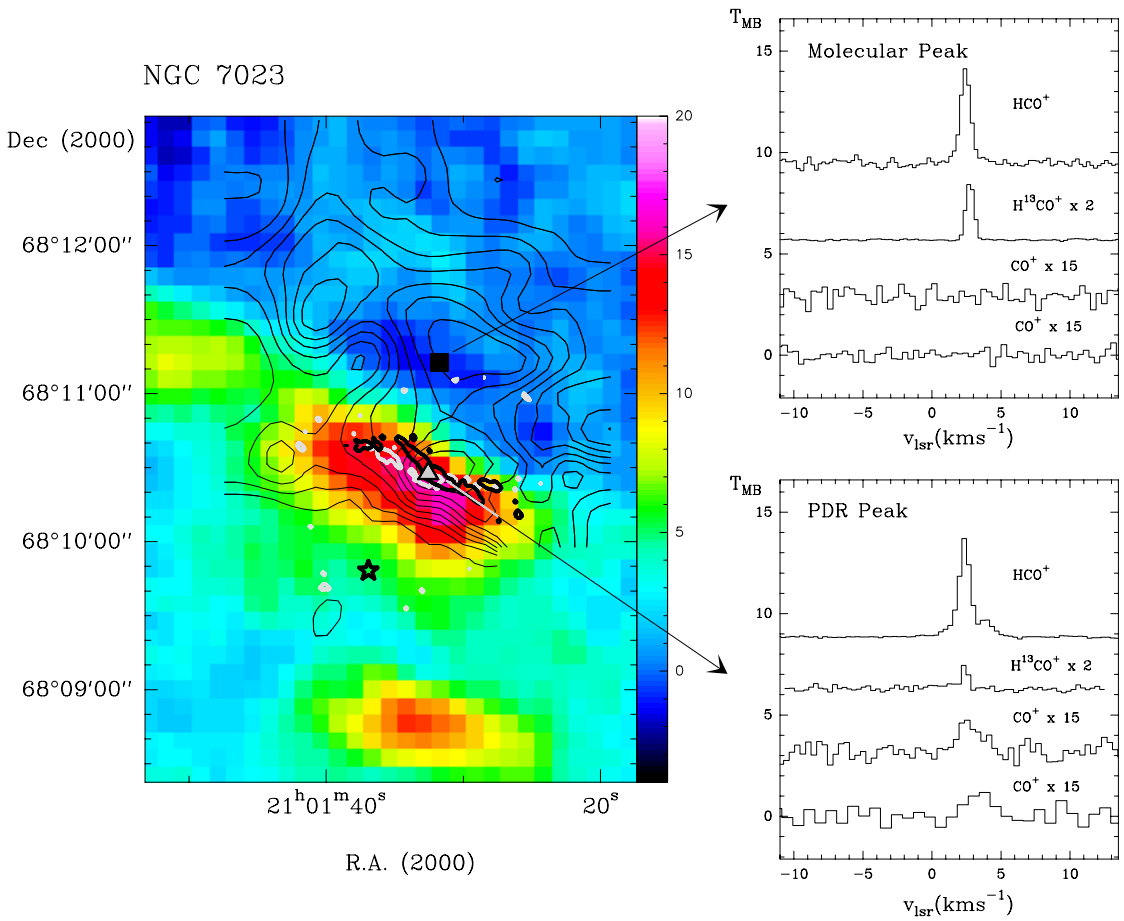

Figure 6. Left panel shows the integrated intensity map of the HCO^+ J=1→0 (solid contours)superposed to the HI column density image (colour map). The HCO^+ molecular filaments as observed with the IRAM PdB interferometer are the heavy contours. On the right we show (top to bottom) the spectra of the HCO^+ J=1→0, $H^{13}CO^+$ J=1→0, and CO^+ N=2→1, J=5/2→3/2 and J=3/2→1/2 lines toward the molecular peak and the PDR peak (taken from Fuente & Martín-Pintado 1997).

5. Summary and final remarks

With FIRST will be able to carry out far-infrared observations with a spatial and angular resolution similar to that achieved by the present large millimeter telescope. The detailed studies of prototypical nearby objects (L1544, L 1157, NGC 7023) will allow us to characterize the physics and chemistry of infall, outflows and PDRs taking full advantage of the spatial and spectral resolution provided by HIFI. These studies will provide diagnostics to be applied to large samples of young stellar objects. Important questions on stellar evolution like, when do energetic outflows start?, when the PDR is developed in the inner envelope?, which is the main mechanism for the dispersal of the envelope and circumstellar disk in pre-main sequence stars?, could find an answer.

Chemical diagnostics will be essential in the study of infall, outflow and PDRs. In particular, the study of the oxygen chemistry, mainly H_2O, in Class 0 and I objects will constitute a key tool for the understanding of the formation and evolution of the infall/outflow system. Phodissociation by the UV stellar radiation could play an essential role in the later stages of the pre-main sequence evolution, Class II and III. The observations of hydrides will be an excellent tracer of the physical conditions and kinematics of PDRs. Because of their peculiar molecular structure the hydrides, as well as water, are not observable from ground-based observatories.

Table 2. List of observable lines

Mol	X_i	$\lambda\mu$m	E_{upper} (K)	A_{ij} (s^{-1})	Exp. Flux[1] (erg s^{-1} cm^{-2})
CO	10^{-5}	186	580	2.9 10^{-4}	1.4 10^{-13}
CH	10^{-6}	149	96	2.2 10^{-2}	8.2 10^{-13}
		558	26	2.1 10^{-4}	1.0 10^{-13}
CH_2	10^{-6}	317	112	5.6 10^{-3}	
C_2H	10^{-8}	572	88	4.8 10^{-4}	7.5 10^{-16}
OH	10^{-6}	119	120	1.4 10^{-1}	5.0 10^{-13}
		163	88	6.5 10^{-2}	5.0 10^{-14}
OH^+	10^{-7}	304	53	1.5 10^{-2}	7.6 10^{-14}
CH^+	10^{-7}	353	41	5.1 10^{-3}	9.5 10^{-14}
HCO^+	10^{-8}	560	89	1.4 10^{-2}	5.2 10^{-14}
CN	10^{-9}	528	81	2.0 10^{-3}	2.0 10^{-17}
CO^+	10^{-9}	635	56	4.1 10^{-3}	2.0 10^{-17}
HCN	10^{-10}	564	89	5.9 10^{-3}	1.0 10^{-16}
CS	10^{-10}	612	129	2.5 10^{-3}	6.0 10^{-18}

[1] Expected flux assuming T_k = 300 K, n = 10^6 cm^{-3}, N_{H_2} = 5 10^{20} cm^{-2}, Δv = 3 kms^{-1}, and Ω_s = 30 ″

Acknowledgements

I thank Dr. Martín-Pintado for his careful reading of the manuscript and Dr. Bachiller for providing Fig. 1 and 4. This work has been partially supported by the Spanish CICYT and the European Commission under grant numbers ESP-1291-E and 1FD1997-1442.

References

Andre P., Ward-Thompson D., Barsony M., 2000, *Protostars and Planets IV* (Book-Tucson: University of Arizona Press; eds Mannings, V., Boss, A.P., Russell, S.S.), p.59

Bachiller R., Pérez Gutiérrez M., Kumar M.S.N. et al., 2001, submmitted to A&A

Bertoldi F., Draine B.T., 1996, ApJ 458, 222

Black J., 1998, *Faraday Discussions, Royal Chemical Society (UK)*, 109, 257

Ceccarelli C., Hollenbach D.J., Tielens A.G.G.M., 1996, ApJ 471, 400

Ceccarelli C., Caux E., Loinard L., 1999, *The Universe as Seen by ISO*, eds. P. Cox & M. F. Kessler. ESA-SP 427.

Cernicharo J., González-Alfonso E., Alcolea J. et al. 1994, ApJ 432, 59

Cernicharo J., Bachiller R., González-Alfonso E., 1996, A&A 305, 5

Cernicharo J., González-Alfonso E., Sempere M.J. et al. 1999, *The Universe as seen by ISO*, Eds. P. Cox & M.F. Kessler, ESA-SP 427

Charnley S.B., 1997, ApJ 481, 396

Kaufman M.J., Neufeld D.A., 1996, ApJ 456, 611

Fuente A., Martín-Pintado J., Gaume R., 1995, ApJ 442, 33

Fuente A. & Martín-Pintado J., 1997, A&A 477, 107

Fuente A., Martín-Pintado J., Bachiller R. et al. 1998, A&A 334, 253

Fuente A., Martín-Pintado J., Rodriguez-Fernández N.J. et al. 1999, ApJ 518, L45

Fuente A., Martín-Pintado J., Rodriguez-Fernández N.J. et al. 2000, A&A 354, 1053

Fuente A., Neri R., Martín-Pintado J. et al. 2001, A&A, in press

Gensheimer P.D., Mauersberger R., Wilson T.L., 1996, A&A 314, 281

González-Alfonso E., Cernicharo J., Bachiller R. et al. 1995, A&A 293, 9

Goran S., Weintraub D.A. 1994, A&A 292, 1

Latter W.B., Walker C.K., Maloney, P.R., 1993, ApJ 419, L97

Hogerheijde M.R., Jansen D.J., van Dishoeck, E.F., 1995, A&A 294, 792

Lemaire J.L., Field D., Maillard J.P. et al. 1999, A&A 349, 253

Liseau R., Ceccarelli C., Larsson B. et al. 1996, A&A 315, L181

Lorenzetti D., Tommasi M., Gianini T. et al. 1999, A&A 346, 604

Martín-Pintado J., Bachiller R., Fuente A., 1992, A&A 254, 315

Menten K., Melnick Gary J., Philips T.G., 1990, ApJ 350, 41

Molinari S., Noriega-Crespo A., Ceccarelli C. et al. 2000, ApJ 538, 698

Myers P.C., Evans N.J.II, Ohashi N., 2000, *Protostars and Planets IV*, Book-Tucson: University of Arizona Press; eds Mannings V., Boss A.P., Russell S.S, p.217

Neufeld D.A., Ashby M.L.N., Bergin E.A. et al. 2000, ApJ 539, 107

Nisini B., Benedettini M., Gianini T. et al. 1999, A&A 350, 529

Saraceno P., Benedettini M., Di Giorgio A.M. et al. 1999, in Physics and Chemistry of the Interstellar Medium III, eds V. Ossenkopf et al. (Berlin: Springer), p. 279

Schilke P., Walmsley M., Pineau Des Forets G. et al., 1997, ApJ, 487, 171

Shu, F.H., 1977, ApJ, 214, 488

Sternberg A., Dalgarno A., 1995, ApJS 99, 565

Störzer H., Hollenbach D., 1998, ApJ 495, 853

van den Ancker, M.E., 1999, PhD Thesis, University of Amsterdam

Zmuidzinas J., Blake, G., Carlstrom J. et al., 1994, AAS 184, 1604